

Harmonic inversion as a general method for periodic orbit quantization

Jörg Main,¹ Vladimir A. Mandelshtam,² Günter Wunner,³ and Howard S. Taylor⁴

¹ Theoretische Physik I, Ruhr-Universität Bochum, D-44780 Bochum, Germany

² University California Irvine, Department of Chemistry, Los Angeles, CA 92612

³ Inst. f. Theor. Physik und Synergetik, Universität Stuttgart, D-70550 Stuttgart, Germany

⁴ University of Southern California, Department of Chemistry, Los Angeles, CA 90089

Abstract. In semiclassical theories for chaotic systems such as Gutzwiller's periodic orbit theory the energy eigenvalues and resonances are obtained as poles of a non-convergent series $g(w) = \sum_n A_n \exp(is_n w)$. We present a general method for the analytic continuation of such a non-convergent series by harmonic inversion of the "time" signal, which is the Fourier transform of $g(w)$. We demonstrate the general applicability and accuracy of the method on two different systems with completely different properties: the Riemann zeta function and the three disk scattering system. The Riemann zeta function serves as a mathematical model for a bound system. We demonstrate that the method of harmonic inversion by filter-diagonalization yields several thousand zeros of the zeta function to about 12 digit precision as eigenvalues of small matrices. However, the method is not restricted to bound and ergodic systems, and does not require the knowledge of the mean staircase function, i.e., the Weyl term in dynamical systems, which is a prerequisite in many semiclassical quantization conditions. It can therefore be applied to open systems as well. We demonstrate this on the three disk scattering system, as a physical example. The general applicability of the method is emphasized by the fact that one does not have to resort a symbolic dynamics, which is, in turn, the basic requirement for the application of cycle expansion techniques.

PACS numbers: 03.65.Sq, 05.45.+b, 02.30.Px

Short title: Harmonic inversion as a general method for periodic orbit quantization

1. Introduction

Since the development of *periodic orbit theory* by Gutzwiller [1, 2] it has become a fundamental question as to how individual semiclassical eigenenergies and resonances can be obtained from periodic orbit quantization for classically chaotic systems. A major problem is the exponential proliferation of the number of periodic orbits with increasing period, resulting in a divergence of Gutzwiller's trace formula at real energies and below the real axis, where the poles of the Green's function are located. The periodic orbit sum is a Dirichlet series

$$g(w) = \sum_n A_n e^{i s_n w} , \quad (1)$$

where the parameters A_n and s_n are the amplitudes and periods (actions) of the periodic orbit contributions. In most applications Eq. 1 is absolutely convergent only in the region $\text{Im } w > c > 0$ with c the entropy barrier of the system, while the poles of $g(w)$, i.e., the bound states and resonances, are located on and below the real axis, $\text{Im } w \leq 0$. Thus, to extract individual eigenstates, the semiclassical trace formula (1) has to be analytically continued to the region of the quantum poles.

Up to now no general procedure is known for the analytic continuation of a non-convergent Dirichlet series of the type of Eq. 1. All existing techniques are restricted to special situations. For bound and ergodic systems the semiclassical eigenenergies can be extracted with the help of a functional equation and the mean staircase function (Weyl term), resulting in a Riemann-Siegel look-alike formula [3, 4, 5, 6]. Alternative semiclassical quantization conditions based on a semiclassical representation of the spectral staircase [7, 8] and derived from a quantum version of a classical Poincaré map [9] are also restricted to bound and ergodic systems.

For systems with a symbolic dynamics the periodic orbit sum (1) can be reformulated as an infinite Euler product, which can be expanded in terms of the cycle length of the symbolic code. If the contributions of longer orbits are shadowed by the contributions of short orbits the cycle expansion technique can remarkably improve the convergence properties of the series and allows to extract the bound states and resonances of bound and open systems, respectively [10, 11, 12, 13]. A combination of the cycle expansion technique with a functional equation for bound systems has been studied by Tanner et al. [14]. However, the existence of a simple symbolic code is restricted to very few systems, and cycle expansion techniques cannot be applied, e.g., to the general class of systems with mixed regular-chaotic classical dynamics.

In this paper we present a general technique for the analytic continuation and the extraction of poles of a non-convergent series of the type of Eq. 1. The method is based on *harmonic inversion* by filter-diagonalization. The advantage of the method is that it does not depend on special properties of the system such as ergodicity or

the existence of a symbolic dynamics for periodic orbits. It does not even require the knowledge of the mean staircase function, i.e., the Weyl term in dynamical systems. The only assumption we have to make is that the analytic continuation of the Dirichlet series $g(w)$ (Eq. 1) is a linear combination of poles $(w - w_k)^{-1}$, which is exactly the functional form of, e.g., a quantum mechanical response function with real and complex parameters w_k representing the bound states and resonances of the system, respectively. To demonstrate the general applicability and accuracy of our method we will apply it to two systems with completely different properties, first the zeros of the Riemann zeta function [15, 16], as a mathematical model for a bound system, and second the three disk scattering system as a physical example.

As pointed out by Berry [3] the density of zeros of Riemann's zeta function can be written, in formal analogy with Gutzwiller's semiclassical trace formula, as a non-convergent series, where the "periodic orbits" are the prime numbers. A special property of this system is the existence of a functional equation which allows the calculation of Riemann zeros via the Riemann-Siegel formula [15, 16, 17]. An analogous functional equation for quantum systems with an underlying chaotic (ergodic) classical dynamics has served as the basis for the development of a semiclassical quantization rule for bound ergodic systems [3, 4, 5, 6]. The Riemann zeta function has also served as a mathematical model to study the statistical properties of level distributions [17, 18, 19]. We will demonstrate that harmonic inversion can reveal the Riemann zeros with extremely high accuracy and with just prime numbers as input data. The most important advantage of our method is, however, its wide applicability, i.e., it can be generalized in a straightforward way to non-ergodic bound or open systems.

Our second example, the three disk scattering problem, is an open and non-ergodic system. Its classical dynamics is purely hyperbolic, and the periodic orbits can be classified by a complete binary symbolic code. This system has served as a model for the development of cycle expansion techniques [10, 12, 13]. When applying the harmonic inversion technique to the three disk scattering system we will highlight the general applicability of our method by not having to make use of its symbolic dynamics in any way.

It is evident that methods invoking special properties of a given system may be more efficient regarding, e.g., the number of periodic orbits required for the calculation of a certain number of poles of the response function $g(w)$ in that particular case. It is not our purpose to compete with the efficiency of such methods. Rather, the advantage of the harmonic inversion technique lies in its wide applicability, which allows the investigation also of systems not possessing special properties. This is demonstrated in this paper by solving two completely different problems, viz. the zeros of the Riemann zeta function and the three disk scattering system, with one and the same method.

The paper is organized as follows. In Section 2 we explain the general idea of the method by way of example of the Riemann zeros. This is followed by the derivation of the harmonic inversion method in Section 3 and the presentation of numerical results for the Riemann zeros in Section 4. The method is extended to the general case of periodic orbit quantization in Section 5, and its usefulness and wide applicability is demonstrated for the three disk scattering system, as a physical example, in Section 6.

2. The Riemann zeta function

Our goal is to introduce our method for periodic orbit quantization by harmonic inversion using, as an example, the well defined problem of calculating zeros of the Riemann zeta function. There are essentially two advantages of studying the zeta function instead of a “real” physical bound system. First, the Riemann analogue of Gutzwiller’s trace formula is exact, as is the case for systems with constant negative curvature [2, 8], whereas the semiclassical trace formula for systems with plane geometry is correct only to first order in \hbar . This allows a direct check on the precision of the method. Second, no extensive periodic orbit search is necessary for the calculation of Riemann zeros, as the only input data are just prime numbers. It is not our intention to introduce yet another method for computing Riemann zeros, which, as an objective in its own right, can be accomplished more efficiently by specific procedures. Rather, in our context the Riemann zeta function serves primarily as a mathematical model to illustrate the power of our technique when applied to bound systems.

2.1. General remarks

Before discussing the harmonic inversion method we start with recapitulating a few brief remarks on Riemann’s zeta function necessary for our purposes. The hypothesis of Riemann is that all the non-trivial zeros of the analytic continuation of the function

$$\zeta(z) = \sum_{n=1}^{\infty} n^{-z} = \prod_p (1 - p^{-z})^{-1}, \quad (\text{Re } z > 1, p : \text{primes}) \quad (2)$$

have real part $\frac{1}{2}$, so that the values $w = w_k$, defined by

$$\zeta\left(\frac{1}{2} - iw_k\right) = 0, \quad (3)$$

are all real or purely imaginary [15, 16]. The Riemann staircase function for the zeros along the line $z = \frac{1}{2} - iw$, defined as

$$N(w) = \sum_{k=1}^{\infty} \Theta(w - w_k), \quad (4)$$

i.e. the number $N(w)$ of zeros with $w_k < w$, can be split [3, 15, 16] into a smooth part,

$$\begin{aligned}\overline{N}(w) &= \frac{1}{\pi} \arg \Gamma \left(\frac{1}{4} + \frac{1}{2} iw \right) - \frac{w}{2\pi} \ln \pi + 1 \\ &= \frac{w}{2\pi} \left(\ln \left\{ \frac{w}{2\pi} \right\} - 1 \right) + \frac{7}{8} + \frac{1}{48\pi w} - \frac{7}{5760\pi w^3} + \mathcal{O}(w^{-5}),\end{aligned}\quad (5)$$

and a fluctuating part,

$$N_{\text{osc}}(w) = -\frac{1}{\pi} \lim_{\eta \rightarrow 0} \text{Im} \ln \zeta \left(\frac{1}{2} - i(w + i\eta) \right). \quad (6)$$

Substituting the product formula (2) (assuming that it can be used when $\text{Re } z = \frac{1}{2}$) into (6) and expanding the logarithms yields

$$N_{\text{osc}}(w) = -\frac{1}{\pi} \text{Im} \sum_p \sum_{m=1}^{\infty} \frac{1}{mp^{m/2}} e^{iwm \ln(p)}. \quad (7)$$

Therefore the density of zeros along the line $z = \frac{1}{2} - iw$ can formally be written as

$$\varrho_{\text{osc}}(w) = \frac{dN_{\text{osc}}}{dw} = -\frac{1}{\pi} \text{Im } g(w) \quad (8)$$

with the response function $g(w)$ given by the series

$$g(w) = i \sum_p \sum_{m=1}^{\infty} \frac{\ln(p)}{p^{m/2}} e^{iwm \ln(p)}, \quad (9)$$

which converges only for $\text{Im } w > \frac{1}{2}$.

Obviously Eq. 9 is of the same type as the response function (1), with the entropy barrier $c = \frac{1}{2}$, i.e., Eq. 9 does not converge on the real axis, where the Riemann zeros are located. The mathematical analogy between the above equation and Gutzwiller's periodic orbit sum

$$\varrho_{\text{osc}}(E) \approx -\frac{1}{\pi} \text{Im} \sum_{\text{po}} \mathcal{A}_{\text{po}} e^{iS_{\text{po}}}, \quad (10)$$

with \mathcal{A}_{po} the amplitudes and S_{po} the classical actions (including phase information) of the periodic orbit contributions, was already pointed out by Berry [3, 4]. For the Riemann zeta function the primitive periodic orbits have to be identified with the primes p , and the integer m formally counts the “repetitions” of orbits. The “amplitudes” and “actions” are then given by

$$\mathcal{A}_{pm} = i \frac{\ln(p)}{p^{m/2}}, \quad (11)$$

$$S_{pm} = mw \ln(p). \quad (12)$$

Both equation (8) for the Riemann zeros and – for most classically chaotic physical systems – the periodic orbit sum (10) do not converge. In particular, zeros of the

zeta function, or semiclassical eigenstates, cannot be obtained directly using these expressions. The problem is to find the analytic continuation of these equations to the region where the Riemann zeros or, for physical systems, the eigenenergies and resonances, are located. Eq. 9 is the starting point for our introduction and discussion of the harmonic inversion technique for the example of the Riemann zeta function. The generalization of the method to periodic orbit quantization (Eq. 10) in Section 5 will be straightforward.

Although Eq. 9 is the starting point for the harmonic inversion method, for completeness we quote the Riemann-Siegel formula, which is the most efficient approach to computing Riemann zeros. For the Riemann zeta function it follows from a functional equation [15] that the function

$$Z(w) = \exp \left\{ -i \left[\arg \Gamma \left(\frac{1}{4} + \frac{1}{2} iw \right) - \frac{1}{2} w \ln \pi \right] \right\} \zeta \left(\frac{1}{2} - iw \right) \quad (13)$$

is real, and even for real w . The asymptotic representation of $Z(w)$ for large w ,

$$\begin{aligned} Z(w) = & -2 \sum_{n=1}^{\text{Int}[\sqrt{w/2\pi}]} \frac{\cos\{\pi \bar{N}(w) - w \ln n\}}{n^{1/2}} \\ & - (-1)^{\text{Int}[\sqrt{w/2\pi}]} \left(\frac{2\pi}{w} \right)^{\frac{1}{4}} \frac{\cos(2\pi(t^2 - t - 1/16))}{\cos(2\pi t)} + \dots, \end{aligned} \quad (14)$$

with $t = \sqrt{w/2\pi} - \text{Int}[\sqrt{w/2\pi}]$ is known as the Riemann-Siegel formula and has been employed (with several more correction terms) in effective methods for computing Riemann zeros [17]. Note that the principal sum in (14) has discontinuities at integer positions of $\sqrt{w/2\pi}$, and therefore the Riemann zeros obtained from the principal sum are correct only to about 1 to 15 percent of the mean spacing between the zeros. The higher order corrections to the principal Riemann-Siegel sum remove, one by one, the discontinuities in successive derivatives of $Z(w)$ at the truncation points and are thus essential to obtaining accurate numerical results. An alternative method for improving the asymptotic representation of $Z(w)$ by smoothing the cut-offs with an error function and adding higher order correction terms is presented in [6].

An analogue of the functional equation for bound and ergodic dynamical systems has been used as the starting point to develop a “rule for quantizing chaos” via a “Riemann-Siegel look-alike formula” [4, 5, 6]. This method is very efficient as it requires the least number of periodic orbits, but unfortunately it is restricted to ergodic systems on principle reasons, and cannot be generalized either to systems with regular or mixed classical dynamics or to open systems.

By contrast, the method of harmonic inversion does not have these restrictions. We will demonstrate that Riemann zeros can be obtained directly from the “ingredients” of the non-convergent response function (9), i.e., the set of values A_{pm} and S_{pm} , thus

avoiding the use of the functional equation, the Riemann-Siegel formula, the mean staircase function (5), or any other special property of the zeta function. The comparison of results in Section 4 will show that the accuracy of our method goes far beyond the Riemann-Siegel formula (14) without higher order correction terms. The main goal of this paper is to demonstrate that because of the formal equivalence between Eqs. (8) and (10) our method can then be applied to periodic orbit quantization of dynamical systems [20] without any modification.

2.2. The ansatz for the Riemann zeros

To find the analytic continuation of Eq. (9) in the region $\text{Im } w < \frac{1}{2}$ we essentially wish to fit $g(w)$ to its exact functional form,

$$g_{\text{ex}}(w) = \sum_k \frac{d_k}{w - w_k + i\epsilon}, \quad (15)$$

arising from the definition of the Riemann staircase (4). The ‘‘multiplicities’’ d_k in Eq. 15 are formally fitting parameters, which here all should be equal to 1.

It is hard to directly adjust the non-convergent (on the real axis) series $g(w)$ to the form of $g_{\text{ex}}(w)$. The first step towards the solution of the problem is to carry out the adjustment for the Fourier components of the response function,

$$C(s) = \frac{1}{2\pi} \int_{-\infty}^{+\infty} g(w) e^{-isw} dw = i \sum_p \sum_{m=1}^{\infty} \frac{\ln(p)}{p^{m/2}} \delta(s - m \ln(p)), \quad (16)$$

which after certain regularizations (see below) is a well-behaved function of s . Due to the formal analogy with the results of periodic orbit theory (see Eqs. 11 and 12), $C(s)$ can be interpreted as the recurrence function for the Riemann zeta function, with the recurrence positions $S_{pm} = m \ln(p)$ and recurrence strengths of periodic orbit returns $A_{pm} = i \ln(p) p^{-m/2}$. The exact functional form which now should be used to adjust $C(s)$ is given by

$$C_{\text{ex}}(s) = \frac{1}{2\pi} \int_{-\infty}^{+\infty} g_{\text{ex}}(w) e^{-isw} dw = -i \sum_{k=1}^{\infty} d_k e^{-iw_k s}. \quad (17)$$

$C_{\text{ex}}(s)$ is a superposition of sinusoidal functions with frequencies † w_k given by the Riemann zeros and amplitudes $d_k = 1$.

Fitting a signal $C(s)$ to the functional form of Eq. (17) with, in general, both complex frequencies w_k and amplitudes d_k is known as *harmonic inversion*, with a large variety of applications in various fields [21, 22, 23, 24, 25]. The harmonic inversion analysis is especially non-trivial if the number of frequencies in the signal $C(s)$ is large, e.g., more

† It is convenient to use the word ‘‘frequencies’’ for w_k referring to the sinusoidal form of $C(s)$. We will also use the word ‘‘poles’’ in the context of the response function $g(w)$.

than a thousand. It is additionally complicated by the fact that the conventional way to perform the spectral analysis by studying the Fourier spectrum of $C(s)$ will bring us back to analyzing the non-convergent response function $g(w)$ defined in Eq. 9. Until recently the known techniques of spectral analysis [21] would not be applicable in the present case. It is the filter-diagonalization method [22, 23, 24] which have turned the harmonic inversion concept into a general and powerful computational tool.

The signal $C(s)$ as defined by Eq. 16 is not yet suitable for the spectral analysis. The next step is to regularize $C(s)$ by convoluting it with a Gaussian function to obtain the smoothed signal,

$$\begin{aligned} C_\sigma(s) &= \frac{1}{\sqrt{2\pi}\sigma} \int_{-\infty}^{+\infty} C(s') e^{-(s-s')^2/2\sigma^2} ds' \\ &= \frac{i}{\sqrt{2\pi}\sigma} \sum_p \sum_{m=1}^{\infty} \frac{\ln(p)}{p^{m/2}} e^{-(s-m \ln(p))^2/2\sigma^2} \end{aligned} \quad (18)$$

that has to be adjusted to the functional form of the corresponding convolution of $C_{\text{ex}}(s)$. The latter is readily obtained by substituting d_k in Eq. 17 by the damped amplitudes,

$$d_k \rightarrow d_k^{(\sigma)} = d_k e^{-w_k^2 \sigma^2 / 2} . \quad (19)$$

The regularization (18) can also be interpreted as a cut of an infinite number of high frequencies in the signal which is of fundamental importance for numerically stable harmonic inversion. Note that the convolution with the Gaussian function is no approximation, and the obtained frequencies w_k and amplitudes d_k corrected by Eq. 19 are still exact, i.e., do not depend on σ . The convolution is therefore not related to the Gaussian smoothing devised for Riemann zeros in [26] and for quantum mechanics in [27], which provides low resolution spectra only.

Before proceeding further we note that even though the derivation of Eq. 18 assumed that the zeros w_k are on the real axis, the analytic properties of $C_\sigma(s)$ imply that its representation by Eq. 18 includes not only the non-trivial real zeros, but also all the trivial ones, $w_k = -i(2k + \frac{1}{2})$, $k = 1, 2, \dots$, which are purely imaginary. The general harmonic inversion procedure described below does not require the frequencies to be real. Both the real and imaginary zeros w_k will be obtained as the eigenvalues of a non-Hermitian generalized eigenvalue problem.

3. Filter-diagonalization method for harmonic inversion

The harmonic inversion problem can be formulated as a non-linear fit (see, e.g., Ref. [21]) of the signal $C(s)$ defined on an equidistant grid,

$$c_n \equiv C(n\tau) = \sum_k d_k e^{-in\tau w_k} , \quad n = 0, 1, 2, \dots, N, \quad (20)$$

with the set of generally complex variational parameters $\{w_k, d_k\}$. (In this context the Discrete Fourier Transform scheme would correspond to a linear fit with N amplitudes d_k and fixed real frequencies $w_k = 2\pi k/N\tau$, $k = 1, 2, \dots, N$. The latter implies the so called ‘‘uncertainty principle’’, i.e., the resolution, defined by the Fourier grid spacing, Δw , is inversely proportional to the length, $s_{\max} = N\tau$, of the signal $C(s)$.) The ‘‘high resolution’’ property associated with Eq. 20 is due to the fact that there is no restriction for the closeness of the frequencies w_k as they are variational parameters. In Ref. [22] it was shown how this non-linear fitting problem can be recast as a linear algebraic one using the filter-diagonalization procedure. The essential idea is to associate the signal c_n with an autocorrelation function of a suitable dynamical system,

$$c_n = (\Phi_0, \hat{U}^n \Phi_0), \quad (21)$$

where (\cdot, \cdot) defines a complex symmetric inner product (i.e., no complex conjugation). The evolution operator can be defined implicitly by

$$\hat{U} \equiv e^{-i\tau\hat{\Omega}} = \sum_{k=1}^K e^{-i\tau\omega_k} |\Upsilon_k\rangle\langle\Upsilon_k|, \quad (22)$$

where the set of eigenvectors $\{\Upsilon_k\}$ is associated with an arbitrary orthonormal basis set and the eigenvalues of \hat{U} are $u_k \equiv e^{-i\tau\omega_k}$ (or equivalently the eigenvalues of $\hat{\Omega}$ are ω_k). Inserting Eq. 22 into Eq. 21 we obtain Eq. 20 with

$$d_k = (\Upsilon_k, \Phi_0)^2, \quad (23)$$

which also implicitly defines the ‘‘initial state’’ Φ_0 .

This construction establishes an equivalence between the problem of extracting spectral information from the signal with the one of diagonalizing the evolution operator $\hat{U} = e^{-i\tau\hat{\Omega}}$ (or the Hamiltonian $\hat{\Omega}$) of the fictitious underlying dynamical system. The filter-diagonalization method is then used for extracting the eigenvalues of the Hamiltonian $\hat{\Omega}$ in any chosen small energy window. Operationally this is done by solving a small generalized eigenvalue problem whose eigenvalues yield the frequencies in a chosen window. The knowledge of the operator $\hat{\Omega}$ itself is not required, as for a properly chosen basis the matrix elements of $\hat{\Omega}$ can be expressed only in terms of c_n . The advantage of the filter-diagonalization procedure is its numerical stability with respect to both the length and complexity (the number and density of the contributing frequencies) of the signal. Here we apply the method of Ref. [23] which is an improvement of the filter-diagonalization method of Ref. [22] in that it allows to significantly reduce the required length of the signal by implementing a different Fourier-type basis with an efficient rectangular filter. Such a basis is defined by choosing a small set of values φ_j in the frequency interval of interest, $\tau\omega_{\min} < \varphi_j < \tau\omega_{\max}$, $j = 1, 2, \dots, J$, and the

maximum order, M , of the Krylov vectors, $\Phi_n = e^{-in\tau\hat{\Omega}}\Phi_0$, used in the Fourier series,

$$\Psi_j \equiv \Psi(\varphi_j) = \sum_{n=0}^M e^{in\varphi_j} \Phi_n \equiv \sum_{n=0}^M e^{in(\varphi_j - \tau\hat{\Omega})} \Phi_0. \quad (24)$$

It is convenient to introduce the notations,

$$U_{jj'}^{(p)} \equiv U^{(p)}(\varphi_j, \varphi_{j'}) = \left(\Psi(\varphi_j), e^{-ip\tau\hat{\Omega}}\Psi(\varphi_{j'}) \right), \quad (25)$$

for the matrix elements of the operator $e^{-ip\tau\hat{\Omega}}$, and $\mathbf{U}^{(p)}$, for the corresponding small $J \times J$ complex symmetric matrix. As such $\mathbf{U}^{(1)}$ denotes the matrix representation of the operator \hat{U} itself and $\mathbf{U}^{(0)}$, the overlap matrix with elements $(\Psi(\varphi_j), \Psi(\varphi_{j'}))$, which is required as the vectors $\Psi(\varphi_j)$ are not generally orthonormal. Now using these definitions we can set up a generalized eigenvalue problem,

$$\mathbf{U}^{(p)}\mathbf{B}_k = e^{-ip\tau\omega_k}\mathbf{U}^{(0)}\mathbf{B}_k, \quad (26)$$

for the eigenvalues $e^{-ip\tau\omega_k}$ of the operator $e^{-ip\tau\hat{\Omega}}$. The column vectors \mathbf{B}_k with elements B_{jk} define the eigenvectors Υ_k in terms of the basis functions Ψ_j as

$$\Upsilon_k = \sum_{j=1}^J B_{jk}\Psi_j, \quad (27)$$

assuming that the Ψ_j 's form a locally complete basis.

The matrix elements (25) can be expressed in terms of the signal c_n , the explicit knowledge of the auxiliary objects $\hat{\Omega}$, Υ_k or Φ_0 is not needed. Indeed, insertion of Eq. 24 into Eq. 25, use of the symmetry property, $(\Psi, \hat{U}\Phi) = (\hat{U}\Psi, \Phi)$, and the definition of c_n , Eq. 21, gives after some arithmetics

$$\begin{aligned} U^{(p)}(\varphi, \varphi') &= (e^{-i\varphi} - e^{-i\varphi'})^{-1} \left[e^{-i\varphi} \sum_{n=0}^M e^{in\varphi'} c_{n+p} \right. \\ &\quad - e^{-i\varphi'} \sum_{n=0}^M e^{in\varphi} c_{n+p} - e^{iM\varphi} \sum_{n=M+1}^{2M} e^{i(n-M-1)\varphi'} c_{n+p} \\ &\quad \left. + e^{iM\varphi'} \sum_{n=M+1}^{2M} e^{i(n-M-1)\varphi} c_{n+p} \right], \quad \varphi \neq \varphi', \\ U^{(p)}(\varphi, \varphi) &= \sum_{n=0}^{2M} (M - |M - n| + 1) e^{in\varphi} c_{n+p}. \end{aligned} \quad (28)$$

(Note that the evaluation of $\mathbf{U}^{(p)}$ requires knowledge of c_n for $n = p, p+1, \dots, N = 2M+p$.)

The solution of the generalized eigenvalue problem (26) is usually done by a singular value decomposition of the matrix $\mathbf{U}^{(0)}$. Each value of p yields a set of frequencies w_k and, due to Eqs. 23, 24 and 27, amplitudes,

$$d_k = \left(\sum_{j=1}^J B_{jk} \sum_{n=0}^M c_n e^{in\varphi_j} \right)^2. \quad (29)$$

Note that Eq. 29 is a functional of the half signal $c_n, n = 1, 2, \dots, M$. Even though in all our applications Eq. 29 yields very good results, here we present an even better expression for the coefficients d_k (see Ref. [24]),

$$\begin{aligned} d_k &= \left[\frac{1}{M+1} \sum_{j=1}^J B_{jk} \left(\Psi(\varphi_j), \Psi(w_k) \right) \right]^2 \\ &\equiv \left[\frac{1}{M+1} \sum_{j=1}^J B_{jk} U^{(0)}(\varphi_j, w_k) \right]^2 \end{aligned} \quad (30)$$

with $U^{(0)}(\varphi_j, w_k)$ defined by Eq. 28. Eq. 30 is a functional of the whole available signal $c_n, n = 0, 1, \dots, 2M$.

The converged w_k and d_k should not depend on p . This condition allows us to identify spurious or non-converged frequencies by comparing the results with different values of p (e.g., with $p = 1$ and $p = 2$). We can define the simplest error estimate ε as the difference between the frequencies w_k obtained from diagonalizations with $p = 1$ and $p = 2$, i.e.

$$\varepsilon = |w_k^{(p=1)} - w_k^{(p=2)}|. \quad (31)$$

4. Riemann zeros by harmonic inversion

We have introduced in Section 2 the method for periodic orbit quantization by harmonic inversion for the example of the Riemann zeta function because this model allows a direct check of the precision of our method. In this Section we present and discuss the numerical results obtained for the Riemann zeros. We also discuss the amount of periodic orbit input data, viz. here the prime numbers, required to obtain converged semiclassical eigenenergies and Riemann zeros, respectively.

4.1. Numerical results

For a numerical demonstration we construct the signal $C_\sigma(s)$ using Eqs. 16 and 18 in the region $s < \ln(10^6) = 13.82$ from the first 78498 prime numbers and with a Gaussian smoothing width $\sigma = 0.0003$. Parts of the signal are presented in Fig. 1. Up to $s \approx 8$ the Gaussian approximations to the δ -functions do essentially not overlap (see Fig. 1a) whereas for $s \gg 8$ the mean spacing Δs between successive δ -functions becomes much less than the Gaussian width $\sigma = 0.0003$ and the signal fluctuates around the mean $\overline{C}(s) = ie^{s/2}$ (see Fig. 1b). From this signal we were able to calculate about 2600 Riemann zeros to at least 12 digit precision. For the small generalized eigenvalue problem (26) we used matrices with dimension $J < 100$. Some Riemann zeros w_k , the corresponding amplitudes d_k , and the estimated errors ε (see Eq. (31)) are given in

Table 1. Within the numerical error the Riemann zeros are real and the amplitudes are consistent with $d_k = 1$ for non-degenerate zeros. To fully appreciate the accuracy of our harmonic inversion technique we note that zeros obtained from the principal sum of the Riemann-Siegel formula (14) deviate by about 1 to 15 percent of the mean spacing from the exact zeros. Including the first correction term in (14) the approximations to the first five zeros read $w_1 = 14.137$, $w_2 = 21.024$, $w_3 = 25.018$, $w_4 = 30.428$, and $w_5 = 32.933$, which still significantly deviates from the exact values (see Table 1). Considering even higher order correction terms the results will certainly converge to the exact zeros. However, the generalization of such higher order corrections to ergodic dynamical systems is a nontrivial task and requires, e.g., the knowledge of the terms in the Weyl series, i.e., the mean staircase function after the constant [6, 29]. The perfect agreement of our results for the w_k with the exact Riemann zeros to full numerical precision is remarkable and clearly demonstrates that harmonic inversion by filter-diagonalization is a very powerful and accurate technique for the analytic continuation and the extraction of poles of a non-convergent series such as Eq. 1.

A few w_k have been obtained (see Table 2) which are definitely not located on the real axis. Except for the first at $w = i/2$ they can be identified with the trivial real zeros of the zeta function at $z = -2n$; $n = 1, 2, \dots$. In contrast to the nontrivial zeros with real w_k , the numerical accuracy for the trivial zeros decreases rapidly with increasing n . The trivial zeros $w_n = -i(2n + \frac{1}{2})$ are the analogue of resonances in open physical systems with widths increasing with n . The fact that the trivial Riemann zeros are obtained emphasizes the general applicability of our method and demonstrates that periodic orbit quantization by harmonic inversion can be applied not only to closed but to open systems as well. The decrease of the numerical accuracy for very broad resonances is a natural numerical consequence of the harmonic inversion procedure [23, 24].

The value $w = i/2$ in Table 2 is special because in this case the amplitude is negative, i.e., $d_k = -1$. Writing the zeta function in the form [16]

$$\zeta\left(\frac{1}{2} - iw\right) = C \prod_k (w - w_k)^{d_k} A(w, w_k) \quad (32)$$

where C is a constant and A a regularizing function which ensures convergence of the product, integer values d_k are the multiplicities of *zeros*. Therefore it is reasonable to relate negative integer values with the multiplicities of *poles*. In fact, $\zeta(z)$ has a simple pole at $z = \frac{1}{2} - iw = 1$ consistent with $w = i/2$ in Table 2.

4.2. Required signal length

We have calculated Riemann zeros by harmonic inversion of the signal $C_\sigma(s)$ (Eq. 18) which uses prime numbers as input. The question arises what are the requirements on the signal $C_\sigma(s)$, in particular what is the required signal length. In other words, how

many Riemann zeros (or semiclassical eigenenergies) can be converged for a given set of prime numbers (or periodic orbits, respectively). The answer can be directly obtained from the requirements on the harmonic inversion technique. In general, the required signal length s_{\max} for harmonic inversion is related to the average density of frequencies $\bar{\varrho}(w)$ by [24]

$$s_{\max} \approx 4\pi\bar{\varrho}(w) . \quad (33)$$

From Eq. 33 the required number of primes (or periodic orbits) can be directly estimated as $\{\# \text{ primes } p \mid \ln p < s_{\max}\}$ or $\{\# \text{ periodic orbits } \mid s_{\text{po}} < s_{\max}\}$. For the special example of the Riemann zeta function the required number of primes to have a given number of Riemann zeros converged can be estimated analytically. With the average density of Riemann zeros derived from (5),

$$\bar{\varrho}(w) = \frac{d\bar{N}}{dw} = \frac{1}{2\pi} \ln\left(\frac{w}{2\pi}\right) \quad (34)$$

we obtain

$$s_{\max} = \ln(p_{\max}) = 2 \ln\left(\frac{w}{2\pi}\right) \Rightarrow p_{\max} = \left(\frac{w}{2\pi}\right)^2 . \quad (35)$$

The number of primes with $p < p_{\max}$ can be estimated from the prime number theorem

$$\pi(p_{\max}) \sim \frac{p_{\max}}{\ln(p_{\max})} = \frac{(w/2\pi)^2}{2 \ln(w/2\pi)} . \quad (36)$$

On the other hand the number of Riemann zeros as a function of w is given by Eq. (5). The estimated number of Riemann zeros which can be obtained by harmonic inversion from a given set of primes is presented in Fig. 2. For example, about 80 zeros ($w < 200$) can be extracted from the short signal $C_{\sigma}(s)$ with $s_{\max} = \ln(1000) = 6.91$ (168 prime numbers) in agreement with the estimates given above. Obviously, in the special case of the Riemann zeta function the efficiency of our method cannot compete with that of the Riemann-Siegel formula method (14) where the number of terms is given by $n_{\max} = \text{Int}[\sqrt{w/2\pi}]$ and, e.g., 5 terms in Eq. 14 would be sufficient to calculate good approximations to the Riemann zeros in the region $w < 200$. Our primary intention is to introduce harmonic inversion by way of example of the zeros of the Riemann zeta function as a *general* tool for periodic orbit quantization, and not to use it as an alternative method for solving the problem of finding most efficiently zeros of the Riemann zeta function.

A functional equation can only be invoked for the semiclassical quantization of *bound* and *ergodic* systems. In this case the required number of periodic orbits can be estimated from the condition $s_{\max} \approx \pi\bar{\varrho}(w)$ [4, 5, 6], which differs by a factor of 4 from the required signal length (33) for harmonic inversion. Periodic orbit quantization by

harmonic inversion will be of particular advantage in situations where special properties such as a functional equation cannot be invoked, e.g., for bound systems with non-ergodic, i.e., regular or mixed classical dynamics, and for open (scattering) systems.

4.3. A remark on the Riemann hypotheses

We conclude this Section with a remark on the famous Riemann hypotheses mentioned in Section 2.1. Applying our method of harmonic inversion to the signal $C_\sigma(s)$ (Eq. 18) the Riemann hypotheses for the *zeros* of the zeta function, $\zeta(z = \frac{1}{2} - iw_k) = 0$, is directly related to an equivalent statement for the *eigenvalues* $e^{-i\tau w_k}$ of the operator $e^{-i\tau\hat{\Omega}}$, i.e., the generalized eigenvalue problem (26). Speculations that the operator $\hat{\Omega}$ can be regarded as the Hamiltonian of a quantum mechanical system have been presented by Berry [3]. Unfortunately, $\hat{\Omega}$ is not known as it is only defined implicitly by way of its matrix representation (28), which is a linear functional of the signal (18). However, the very fact that the Riemann zeros are obtained as eigenvalues of some matrix with analytically known coefficients is already intriguing.

5. Periodic orbit quantization

As mentioned in Section 2 the basic equation (9) used for the calculation of Riemann zeros has the same mathematical form as Gutzwiller's semiclassical trace formula. Both series, Eq. 9 and the periodic orbit sum (10), suffer from similar convergence problems in that they are absolutely convergent only in the complex half-plane outside the region where the Riemann zeros, or quantum eigenvalues, respectively, are located. As a consequence, in a direct summation of periodic orbit contributions smoothing techniques must be applied resulting in low resolution spectra for the density of states [27, 30]. To extract individual eigenstates the semiclassical trace formula has to be analytically continued to the region of the quantum poles. Here dynamical zeta functions have turned out to be of particular interest.

For *bound* and *ergodic* systems one technique is to apply an approximate functional equation and generalize the Riemann-Siegel formula (14) to dynamical zeta functions [4, 5, 6]. The Riemann-Siegel look-alike formula has been applied, e.g., for the semiclassical quantization of the hyperbola billiard [29]. For bound ergodic systems alternative semiclassical quantization conditions based on a semiclassical representation of the spectral staircase $\mathcal{N}(E) = \sum_n \Theta(E - E_n)$ [7, 8] and derived from a quantum version of a classical Poincaré map [9] have also been discussed.

These quantization techniques cannot be applied to *open* systems. However, if a symbolic dynamics for the system exists, i.e., if the periodic orbits can be classified with the help of a complete symbolic code, the dynamical zeta function, given as an infinite Euler product over entries from classical periodic orbits can be expanded in terms of

the cycle length of the orbits [10, 11]. The *cycle expansion* series is rapidly convergent if the contributions of long orbits are approximately shadowed by contributions of short orbits. The cycle expansion technique has been applied, e.g., to the three disk scattering system [10, 12, 13], the three body Coulomb system [31, 32], and to the hydrogen atom in a magnetic field [33]. A combination of the cycle-expansion method with a functional equation has been applied to bound systems in [14, 34]. However, the existence of a complete symbolic dynamics is more the exception than the rule, and the cycle expansion cannot be applied, in particular for systems with mixed regular-chaotic classical dynamics.

In this Section we apply the same technique that we used for the calculation of Riemann zeros, to the calculation of semiclassical eigenenergies and resonances of physical systems by harmonic inversion of Gutzwiller's periodic orbit sum for the propagator. The method only requires the knowledge of all orbits up to a sufficiently long but finite period and does not rely on either an approximate semiclassical functional equation, nor does it depend on the existence of a symbolic code for the orbits. The method will therefore allow the investigation of a large variety of systems with an underlying chaotic, mixed, or even regular classical dynamics. The derivation of an expression for the recurrence function to be harmonically inverted is analogous to that in Section 2.2.

5.1. Semiclassical density of states

Following Gutzwiller [1, 2] the semiclassical response function for chaotic systems is given by

$$g^{\text{sc}}(E) = g_0^{\text{sc}}(E) + \sum_{\text{po}} \mathcal{A}_{\text{po}} e^{iS_{\text{po}}} , \quad (37)$$

where $g_0^{\text{sc}}(E)$ is a smooth function and the S_{po} and \mathcal{A}_{po} are the classical actions and weights (including phase information given by the Maslov index) of periodic orbit contributions. Eq. (37) is also valid for integrable [35] and near-integrable [36, 37] systems but with different expressions for the amplitudes \mathcal{A}_{po} . It should also be possible to include complex “ghost” orbits [38, 39] and uniform semiclassical approximations [40, 41] close to bifurcations of periodic orbits in the semiclassical response function (37). The eigenenergies and resonances are the poles of the response function but, unfortunately, its semiclassical approximation (37) does not converge in the region of the poles, whence the problem is the analytic continuation of $g^{\text{sc}}(E)$ to this region.

In the following we make the (weak) assumption that the classical system has a scaling property, i.e., the shape of periodic orbits does not depend on the scaling parameter, w , and the classical action scales as

$$S_{\text{po}} = w s_{\text{po}} . \quad (38)$$

Examples of scaling systems are billiards [10, 42], Hamiltonians with homogeneous potentials [43, 44], Coulomb systems [32], or the hydrogen atom in external magnetic and electric fields [45, 33]. Eq. 38 can even be applied for non-scaling, e.g., molecular systems if a generalized scaling parameter $w \equiv \hbar_{\text{eff}}^{-1}$ is introduced as a new dynamical variable [46]. Quantization yields bound states or resonances, w_k , for the scaling parameter. In scaling systems the semiclassical response function $g^{\text{sc}}(w)$ can be Fourier transformed easily to obtain the semiclassical trace of the propagator

$$C^{\text{sc}}(s) = \frac{1}{2\pi} \int_{-\infty}^{+\infty} g^{\text{sc}}(w) e^{-isw} dw = \sum_{\text{po}} \mathcal{A}_{\text{po}} \delta(s - s_{\text{po}}) . \quad (39)$$

The signal $C^{\text{sc}}(s)$ has δ -peaks at the positions of the classical periods (scaled actions) $s = s_{\text{po}}$ of periodic orbits and with peak heights (recurrence strengths) \mathcal{A}_{po} , i.e., $C^{\text{sc}}(s)$ is Gutzwiller's periodic orbit recurrence function. Consider now the quantum mechanical counterparts of $g^{\text{sc}}(w)$ and $C^{\text{sc}}(w)$ taken as the sums over the poles w_k of the Green's function,

$$g^{\text{qm}}(w) = \sum_k \frac{d_k}{w - w_k + i\epsilon} , \quad (40)$$

$$C^{\text{qm}}(s) = \frac{1}{2\pi} \int_{-\infty}^{+\infty} g^{\text{qm}}(w) e^{-isw} dw = -i \sum_k d_k e^{-iw_k s} , \quad (41)$$

with d_k being the multiplicities of resonances, i.e., $d_k = 1$ for non-degenerate states. In analogy with the calculation of Riemann zeros from Eq. (18) the frequencies, w_k , and amplitudes, d_k , can now be extracted by harmonic inversion of the signal $C^{\text{sc}}(s)$ after convoluting it with a Gaussian function, i.e.,

$$C_{\sigma}^{\text{sc}}(s) = \frac{1}{\sqrt{2\pi}\sigma} \sum_{\text{po}} \mathcal{A}_{\text{po}} e^{(s-s_{\text{po}})^2/2\sigma^2} . \quad (42)$$

By adjusting $C_{\sigma}^{\text{sc}}(s)$ to the functional form of Eq. 41, the frequencies, w_k , can be interpreted as the semiclassical approximation to the poles of the Green's function in (40). Note that the harmonic inversion method described in Section 3 allows studying signals with complex frequencies w_k as well. For open systems the complex frequencies can be interpreted as semiclassical resonances. Note also that the w_k in general differ from the exact quantum eigenvalues because Gutzwiller's trace formula (37) is an approximation, correct only to first order in \hbar . Therefore the diagonalization of small matrices in (26) does not imply that the results of periodic orbit quantization are more "quantum" in any sense than those obtained, e.g., from a cycle expansion [10, 11]. The eigenvalues are solutions of non-linear equations and the diagonalization is equivalent to the search of zeros of the dynamical zeta function in the cycle expansion technique. Numerical calculation of the zeros is also a non-linear problem and, in contrast to the matrix diagonalization, might encounter a problem of missing roots.

5.2. Semiclassical matrix elements

The procedure described above can be generalized in a straightforward manner to the calculation of semiclassical diagonal matrix elements $\langle \psi_k | \hat{A} | \psi_k \rangle$ of a smooth Hermitian operator \hat{A} . In this case we start from the quantum mechanical trace formula [47]

$$g_A^{\text{qm}}(w) = \text{tr} G^+ \hat{A} = \sum_k \frac{\langle \psi_k | \hat{A} | \psi_k \rangle}{w - w_k + i\epsilon}, \quad (43)$$

which has the same functional form as (40), but with $d_k = \langle \psi_k | \hat{A} | \psi_k \rangle$ instead of $d_k = 1$. For the quantum response function $g_A^{\text{qm}}(w)$ (Eq. 43) a semiclassical approximation has been derived in [47], which has the same form as Gutzwiller's trace formula (37) but with amplitudes

$$\mathcal{A}_{\text{po}} = -i \frac{A_p e^{-i\frac{\pi}{2}\mu_{\text{po}}}}{\sqrt{|\det(M_{\text{po}} - I)|}} \quad (44)$$

where M_{po} is the monodromy matrix and μ_{po} the Maslov index of the periodic orbit, and

$$A_p = \int_0^{S_p} A(\mathbf{q}(s), \mathbf{p}(s)) ds \quad (45)$$

is the classical average of the observable A over *one* period S_p of the *primitive* periodic orbit. Note that $\mathbf{q}(s)$ and $\mathbf{p}(s)$ are functions of the classical action instead of time for scaling systems [48]. Gutzwiller's trace formula for the density of states is obtained with \hat{A} being the identity operator, i.e., $A_p = S_p$. When the semiclassical signal $C^{\text{sc}}(s)$ (Eq. 39) with amplitudes \mathcal{A}_{po} given by Eqs. 44 and 45 is analyzed with the method of harmonic inversion the frequencies and amplitudes obtained are the semiclassical approximations to the eigenvalues w_k and matrix elements $d_k = \langle \psi_k | \hat{A} | \psi_k \rangle$, respectively.

6. The three disk scattering system

Let us consider a billiard system consisting of three identical hard disks with unit radii, $R = 1$, displaced from each other by the same distance d . This simple, albeit nontrivial, scattering system has served as a model for periodic orbit quantization in many investigations in recent years [49, 10, 12, 13]. After symmetry reduction the periodic orbits can be classified by a binary symbolic code [10]. For $d > 2.1$ there is a one-to-one identity between the periodic orbits and the symbolic code, whereas for $d < 2.1$ pruning of orbits sets in. For $d = 6$ semiclassical resonances were calculated by application of the cycle expansion technique including all periodic orbits up to cycle length $n = 13$ [13]. In order to demonstrate the usefulness of the harmonic inversion technique we first apply it to the case $R : d = 1 : 6$ studied before. Note that the ratio corresponds to the very favorable regime for the cycle expansion (see below). In

billiards the scaled action s is given by the length L of orbits ($s = L$) and the quantized parameter is the absolute value of the wave vector $k = |\mathbf{k}| = \sqrt{2mE}/\hbar$. Fig. 3a shows the periodic orbit recurrence function, i.e., the trace of the semiclassical propagator $C^{\text{sc}}(L)$. The groups with oscillating sign belong to periodic orbits with adjacent cycle lengths. To obtain a smooth function on an equidistant grid, which is required for the harmonic inversion method, the δ -functions in (39) have been convoluted with a Gaussian function of width $\sigma = 0.0015$. As explained in Section 2 this does not change the underlying spectrum. The results of the harmonic inversion analysis of this signal are presented in Fig. 3b and Table 3. The crosses in Fig. 3b represent semiclassical poles, for which the amplitudes d_k are very close to 1, mostly within one percent. Because the amplitudes converge much slower than the frequencies these resonance positions can be assumed to be very accurate within the semiclassical approximation. In fact, a perfect agreement to many significant figures is achieved for these poles with the results obtained by cycle expansion [13], and this agreement confirms that the results in Fig. 3b and Table 3 are the true semiclassical resonances, i.e., deviations from the exact quantum poles are solely due to the semiclassical approximation in Gutzwiller's trace formula. For some broad resonances marked by diamonds in Fig. 3b and Table 3 the d_k deviate strongly from 1, within 5 to maximal 50 percent. It is not clear whether these strong deviations are due to numerical effects, such as convergence problems caused by too short a signal, or if they are a direct consequence of the semiclassical approximation. Of course, in the exact expression (41) all multiplicities d_k are 1, but there is no proof that this is still true within the semiclassical approximation. However, for the lowest k eigenvalues (see, e.g., the first three resonances in Table 3), where the agreement with the exact resonance energies is worst [13] $d_k = 1$ still holds, indicating that there is no \hbar -dependence for the multiplicities.

The cycle expansion technique is based on the idea that the contributions of long periodic orbits are shadowed by those of short orbits. For the three disk scattering system this is ideally fulfilled in the limit of a large ratio $d/R \gg 2$. This is no longer true for short distances between the disks and hence the convergence of the conventional cycle expansion becomes rather slow [12]. As a second example of periodic orbit quantization by harmonic inversion we therefore study the three disk scattering system with a short distance ratio $d/R = 2.5$, and thus in a situation where the assumption of the cycle expansion that contributions of long orbits are shadowed by short orbits is no longer a good approximation. The results are presented in Fig. 4 and Table 4. For large L groups of orbits with the same cycle length of the symbolic code strongly overlap and cannot be recognized in Fig. 4a. The signal is obtained from periodic orbits with cycle length $n \leq 13$. Note that only 356 periodic orbits with $L < 7.5$ are included in the signal (Fig. 4a) whereas the complete set of orbits with cycle length $n \leq 13$ consists of 1377 orbits. The resonances obtained by harmonic inversion of the semiclassical recurrence function

are in good agreement with results of the cycle expansion [50].

We finally remark that when a symbolic dynamics exists and contributions of long orbits are shadowed by short orbits the cycle expansion techniques are very efficient and, e.g., for the three disk scattering system with $d \geq 6R$ a large number of resonances can be obtained from just 8 periodic orbits with cycle length $n \leq 4$. Again, we do not aim at competing with the efficiency of the cycle expansion method in such ideal situations. As already mentioned in Section 4 the advantage of periodic orbit quantization by harmonic inversion is its *general* applicability: it does not depend on the existence of a symbolic code and the shadowing of orbits. We have extracted the semiclassical resonances of the three disk scattering problem directly from the periodic orbits with exactly the same method as the Riemann zeros in Section 4 from the primes as 'periodic orbits', for which no symbolic dynamics exists.

7. Conclusion

We have introduced harmonic inversion as a new and general tool for semiclassical periodic orbit quantization. The method requires the complete set of periodic orbits up to a given maximum period as input but does not depend on special properties of the orbits, as, e.g., the existence of a symbolic code or a functional equation. We have demonstrated the wide applicability of the method by applying it to two systems with completely different properties, namely the zeros of the Riemann zeta function and the three disk scattering problem. Both systems have been treated before by efficient methods, which, however, are restricted to bound ergodic systems or systems with a complete symbolic dynamics. The harmonic inversion technique allows to solve both problems with one and the same method. Therefore the method can also serve as a tool for, e.g., the semiclassical quantization of systems with mixed regular-chaotic classical dynamics, which still is a challenging and unsolved problem. The signal $C^{\text{sc}}(s)$ can be composed as the sum of a signal related to the irregular part of the classical phase space with periodic orbit amplitudes given by Gutzwiller's trace formula [2] and a signal related to stable [35] or nearly integrable [36] torus structures. It should also be possible to include, e.g., creeping orbits [51], ghost orbit contributions [38, 39, 25], and higher order \hbar corrections [52] into the signal $C^{\text{sc}}(s)$, which can then be inverted to reveal the semiclassical poles. The method can even be used for a semiclassical periodic orbit quantization of systems with non-homogeneous potentials such as the potential surfaces of molecules when a generalized scaling technique [46] is applied.

Acknowledgments

We are grateful to B. Eckhardt who kindly communicated to us his periodic orbits for the three disk scattering system. J. M. thanks the Alexander von Humboldt-Stiftung for a Feodor-Lynen scholarship and H. Taylor and the University of Southern California for their kind hospitality and support.

References

- [1] Gutzwiller M C 1967 *J. Math. Phys.* **8** 1979 and 1971 *J. Math. Phys.* **12** 343
- [2] Gutzwiller M C 1990, *Chaos in Classical and Quantum Mechanics* (New York: Springer)
- [3] Berry M V 1986, Riemann's zeta function: A model for quantum chaos? *Quantum Chaos and Statistical Nuclear Physics*, ed T H Seligman and H Nishioka (*Lecture Notes in Physics* **263**) (Berlin: Springer) pp 1-17
- [4] Berry M V and Keating J P 1990 *J. Phys. A* **23** 4839
- [5] Keating J 1992 *Chaos* **2** 15
- [6] Berry M V and Keating J P 1992 *Proc. Roy. Soc. Lond. A* **437** 151
- [7] Aurich R, Matthies C, Sieber M and Steiner F 1992, *Phys. Rev. Lett.* **68** 1629
- [8] Aurich R and Bolte J 1992 *Mod. Phys. Lett. B* **6** 1691
- [9] Bogomolny E B 1992 *Nonlinearity* **5** 805
- [10] Cvitanović P and Eckhardt B 1989 *Phys. Rev. Lett.* **63** 823
- [11] Artuso R, Aurell E and Cvitanović P 1990 *Nonlinearity* **3** 325; 361
- [12] Eckhardt B and Russberg G 1993 *Phys. Rev. E* **47** 1578
- [13] Eckhardt B, Cvitanović P, Rosenqvist P, Russberg G and Scherer P 1995 Pinball Scattering, in *Quantum Chaos*, ed G Casati and B V Chirikov, (Cambridge: University Press), pp 405-434
- [14] Tanner G, Scherer P, Bogomolny E B, Eckhardt B and Wintgen D 1991 *Phys. Rev. Lett.* **67** 2410
- [15] Edwards H M 1974 *Riemann's Zeta function* (New York: Academic Press)
- [16] Titchmarsh E C 1986 *The Theory of the Riemann Zeta-Function* OUP, 2nd ed.
- [17] Odlyzko A M 1990 *The 10²⁰th zero of the Riemann zeta function and 70 million of its neighbours* (AT&T Bell Laboratories)
- [18] Bohigas O and Giannoni M J 1984 Chaotic motion and random-matrix theories *Mathematical and Computational Methods in Nuclear Physics* ed J S Dehesa J M G Gomez and A Polls (*Lecture Notes in Physics* **209**) (Berlin: Springer) pp 1-99
- [19] Bogomolny E and Keating J 1995 *Nonlinearity* **8** 1115
- [20] Main J, Mandelshtam V A and Taylor H S 1997 *Phys. Rev. Lett.* **79** 825
- [21] Marple S, Jr. 1987, *Digital Spectral Analysis with Applications*, Prentice-Hall, Englewood Cliffs
- [22] Wall M R and Neuhauser D 1995 *J. Chem. Phys.* **102** 8011
- [23] Mandelshtam V A and Taylor H S 1997 *Phys. Rev. Lett.* **78** 3274
- [24] Mandelshtam V A and Taylor H S 1997 *J. Chem. Phys.* **107** 6756
- [25] Main J, Mandelshtam V A and Taylor H S 1997 *Phys. Rev. Lett.* **78** 4351
- [26] Delsarte J 1966 *J. Anal. Math. (Jerusalem)* **17** 419
- [27] Aurich R, Sieber M and Steiner F 1988 *Phys. Rev. Lett.* **61** 483
- [28] Sieber M and Steiner F 1991 *Phys. Rev. Lett.* **67** 1941
- [29] Keating J P and Sieber M 1994 *Proc. R. Soc. Lond. A* **447** 413

- [30] Wintgen D 1988 *Phys. Rev. Lett.* **61** 1803
- [31] Ezra G S, Richter K, Tanner G and Wintgen D 1991 *J. Phys. B* **24** L413
- [32] Wintgen D, Richter K and Tanner G 1992 *Chaos* **2** 19
- [33] Tanner G, Hansen K T and Main J 1996 *Nonlinearity* **9** 1641
- [34] Tanner G and Wintgen D 1992 *Chaos* **2** 53
- [35] Berry M V and Tabor M 1976 *Proc. R. Soc. London* **A349** 101
- [36] Tomsovic S, Grinberg M and Ullmo D 1995 *Phys. Rev. Lett.* **75** 4346
- [37] Ullmo D, Grinberg M and Tomsovic S 1996 *Phys. Rev. E* **54** 136
- [38] Kuś M, Haake F and Delande D 1993 *Phys. Rev. Lett.* **71** 2167
- [39] Main J and Wunner G 1997 *Phys. Rev. A* **55** 1743
- [40] Ozorio de Almeida A M and Hannay J H 1987 *J. Phys. A* **20** 5873
- [41] Main J and Wunner G 1998 *Phys. Rev. E* **57** in press
- [42] Heller E J 1984 *Phys. Rev. Lett.* **53** 1515
- [43] Martens C C, Waterland R L and Reinhardt W P 1989 *J. Chem. Phys.* **90** 2328
- [44] Tomsovic S 1991 *J. Phys. A* **24** L733
- [45] Main J, Wiebusch G, Welge K H, Shaw J and Delos J B 1994 *Phys. Rev. A* **49** 847
- [46] Main J, Jung C and Taylor H S 1997 *J. Chem. Phys.* **107** 6577
- [47] Eckhardt B, Fishman S, Müller K and Wintgen D 1992 *Phys. Rev. A* **45** 3531
- [48] Boosé D, Main J, Mehlig B and Müller K 1995 *Europhys. Lett.* **32** 295
- [49] Gaspard P and Rice S A 1989 *J. Chem. Phys.* **90** 2225, 2242, and 2255
- [50] Wirzba A, private communication
- [51] Wirzba A 1992 *Chaos* **2** 77
- [52] Gaspard P and Alonso D 1993 *Phys. Rev. A* **47** R3468

Figures and Tables

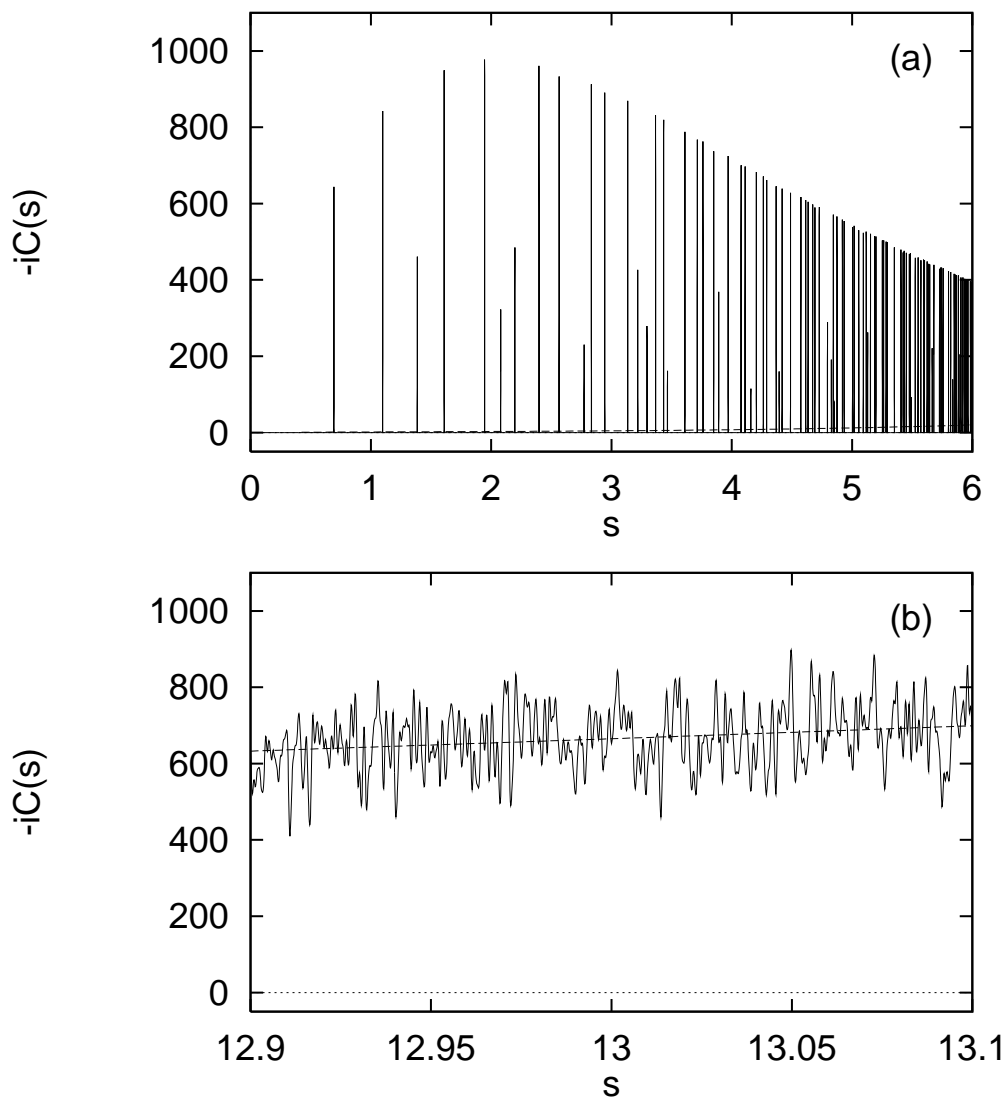


Figure 1. “Recurrence” function $-iC_\sigma(s)$ for the Riemann zeros which has been analyzed by harmonic inversion. (a) Range $0 \leq s \leq 6$, (b) short range around $s = 13$. The δ -functions have been convoluted by a Gaussian with width $\sigma = 0.0003$. Dashed line: Smooth background $\overline{C}(s) = ie^{s/2}$ resulting from the pole of the zeta function.

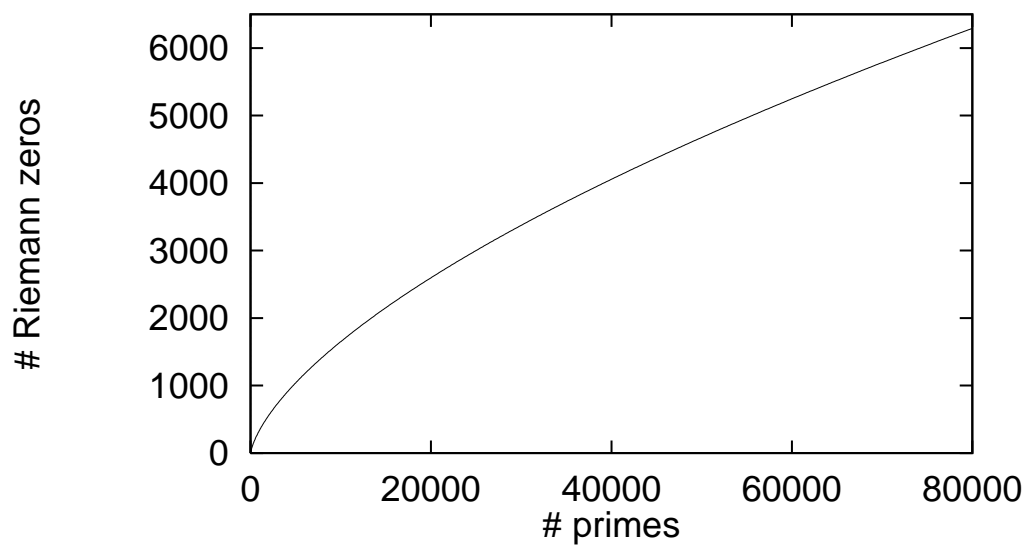


Figure 2. Estimated number of converged zeros of the Riemann zeta function, which can be obtained by harmonic inversion for given number of primes p .

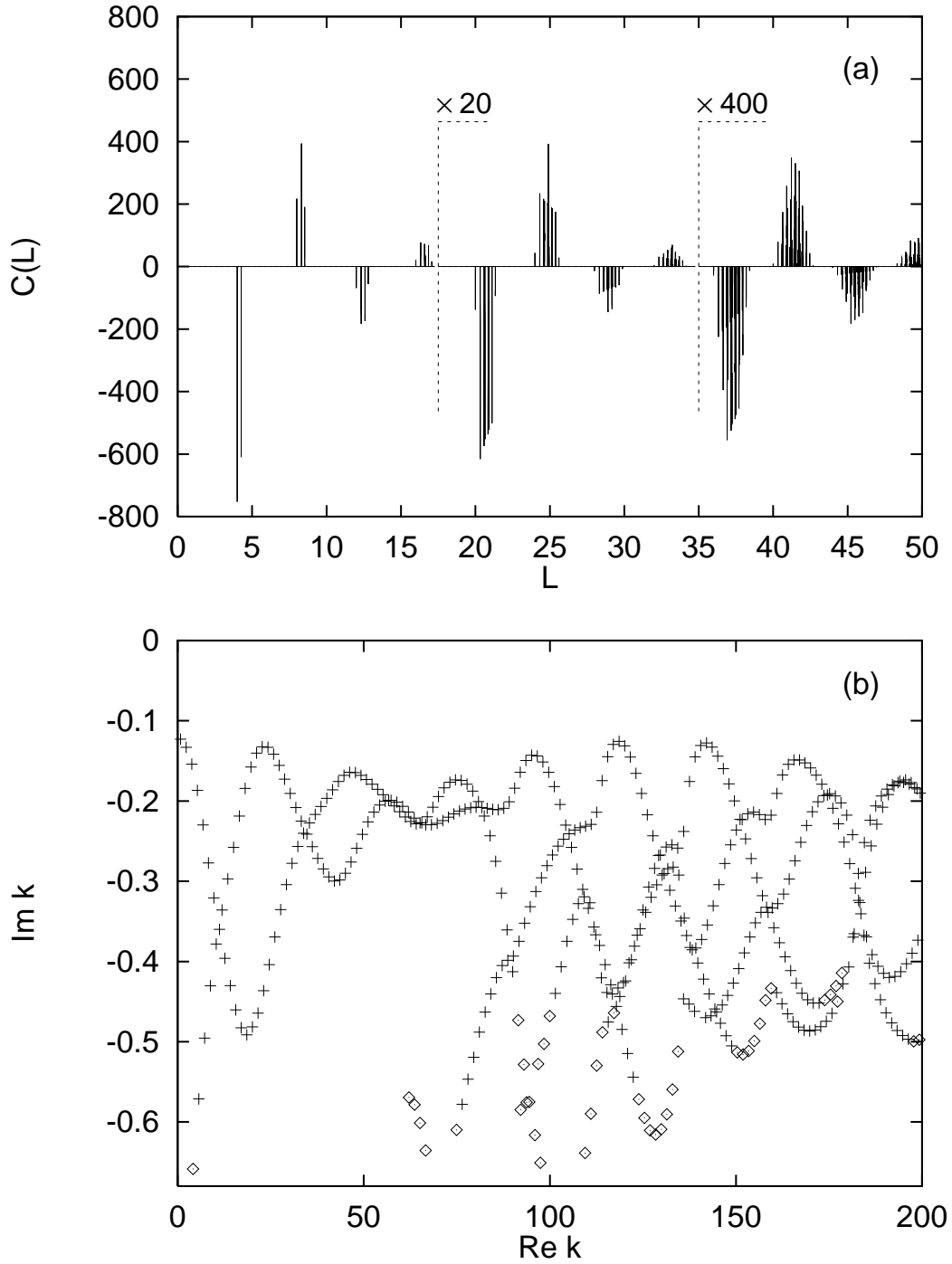


Figure 3. Three disk scattering system (A_1 subspace) with $R = 1$, $d = 6$. (a) Periodic orbit recurrence function, $C(L)$. The signal has been convoluted with a Gaussian of width $\sigma = 0.0015$. (b) Semiclassical resonances. The resonance positions marked by diamonds might be less accurate (see text).

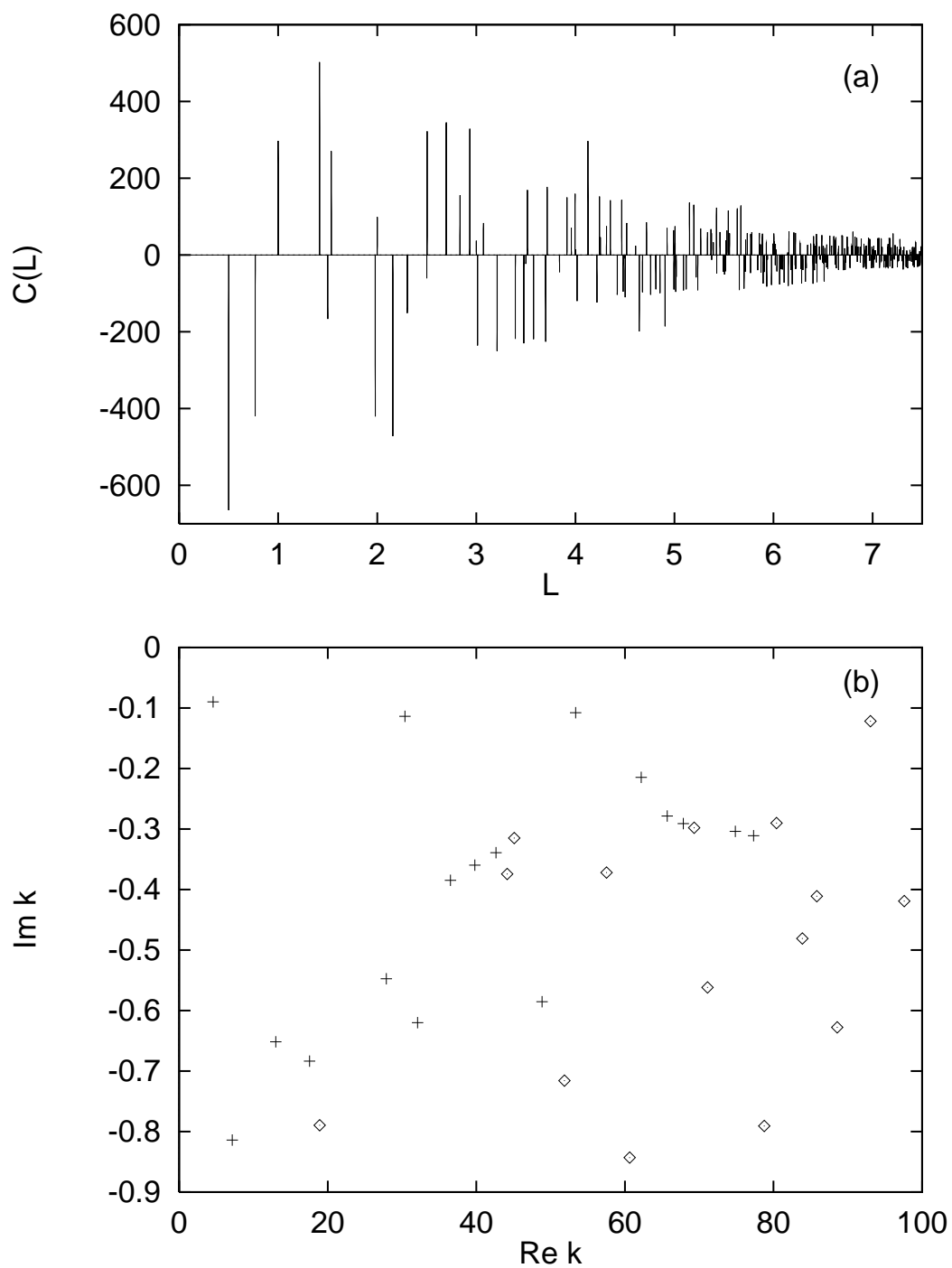


Figure 4. Three disk scattering system (A_1 subspace) with $R = 1$, $d = 2.5$. (a) Periodic orbit recurrence function, $C(L)$. The signal has been convoluted with a Gaussian of width $\sigma = 0.0003$. (b) Semiclassical resonances. The resonance positions marked by diamonds might be less accurate (see text).

Table 1. Non-trivial zeros w_k , multiplicities d_k , and error estimate ε for the Riemann zeta function.

k	Re w_k	Im w_k	Re d_k	Im d_k	ε
1	14.13472514	4.05E-12	1.00000011	-5.07E-08	3.90E-13
2	21.02203964	-2.23E-12	1.00000014	1.62E-07	9.80E-13
3	25.01085758	1.66E-11	0.99999975	-2.64E-07	5.20E-12
4	30.42487613	-6.88E-11	0.99999981	-1.65E-07	1.90E-12
5	32.93506159	7.62E-11	1.00000020	5.94E-08	7.10E-13
6	37.58617816	1.46E-10	1.00000034	5.13E-07	1.00E-12
7	40.91871901	-3.14E-10	0.99999856	1.60E-06	4.90E-11
8	43.32707328	1.67E-11	1.00000008	3.29E-07	1.90E-12
9	48.00515088	4.35E-11	0.99999975	-1.35E-07	1.40E-12
10	49.77383248	7.02E-11	1.00000254	-4.59E-07	1.10E-10
11	52.97032148	1.92E-10	1.00000122	7.31E-07	6.00E-11
12	56.44624770	-1.30E-10	0.99999993	4.51E-07	5.50E-12
13	59.34704400	5.40E-11	0.99999954	2.34E-06	2.30E-10
14	60.83177852	-3.94E-10	1.00000014	1.11E-06	3.00E-11
15	65.11254406	-4.98E-09	0.99998010	-8.30E-06	2.70E-08
...
2551	3083.36135798	8.43E-10	0.99999923	3.45E-07	1.50E-11
2552	3084.83845150	2.72E-09	1.00000057	-2.86E-06	1.80E-10
2553	3085.37726898	-1.37E-08	0.99999576	-2.88E-06	5.50E-10
2554	3085.96552225	6.39E-09	0.99999667	1.50E-06	2.80E-10
2555	3087.01881535	3.46E-11	0.99999845	-3.63E-07	5.20E-11
2556	3088.08343703	-3.89E-10	0.99999931	-8.44E-07	2.40E-11
2557	3089.22230894	-3.31E-10	1.00000017	-9.21E-07	1.80E-11
2558	3090.28219490	2.97E-10	1.00000069	-7.17E-07	2.10E-11
2559	3091.15446969	1.10E-09	1.00000052	-6.59E-07	1.50E-11
2560	3092.68766704	2.25E-09	1.00000033	1.45E-06	5.20E-11
2561	3093.18544571	-2.33E-09	1.00000168	-1.50E-07	6.40E-11
2562	3094.83306842	2.07E-08	0.99999647	2.63E-06	4.20E-10
2563	3095.13203122	-1.79E-08	1.00000459	1.70E-06	5.20E-10
2564	3096.51548551	5.15E-09	0.99999868	2.74E-06	2.20E-10
2565	3097.34260655	7.75E-09	0.99999918	5.12E-06	6.00E-10
2566	3098.03835498	-2.14E-08	1.00000296	4.34E-06	6.20E-10

Table 2. Trivial zeros and pole of the Riemann zeta function.

Re w_k	Im w_k	Re d_k	Im d_k	ε
0.00000000	0.50000000	-1.00000002	-4.26E-08	1.80E-14
-0.00000060	-2.49999941	0.99992487	-3.66E-05	1.80E-07
-0.00129915	-4.49987911	1.00069939	-3.25E-03	4.40E-05
-0.09761173	-6.53286064	1.07141445	-1.49E-01	1.70E-03

Table 3. Semiclassical resonances, multiplicities, and error estimates for the three disk scattering problem (A_1 subspace) with $R = 1$, $d = 6$. The marked resonances are plotted as diamonds in Fig. 3b.

	Re k	Im k	Re d	Im d	ε
	0.75831390	-0.12282220	0.99999998	-0.00000001	2.84E-12
	2.27427857	-0.13305873	1.00000000	0.00000000	2.71E-14
	3.78787678	-0.15412739	1.00000001	0.00000000	1.11E-13
◇	4.14568980	-0.65853972	0.94261284	-0.05782200	1.79E-06
	5.29606778	-0.18678731	1.00000000	0.00000004	2.63E-12
	5.68149760	-0.57137210	0.99512763	-0.01739098	5.34E-07
	6.79363653	-0.22992212	0.99999994	0.00000018	1.54E-11
	7.22405797	-0.49542427	1.00092001	-0.00461967	4.02E-07
	8.27639062	-0.27708051	1.00000064	-0.00000007	3.47E-11
	8.77921337	-0.43025611	0.99900081	0.00120544	1.00E-07
	9.74763287	-0.32081704	0.99999986	0.00000049	6.32E-12
	10.34422566	-0.37819884	1.00000189	0.00001109	3.89E-10
	11.21347781	-0.35996394	1.00000180	-0.00000402	3.87E-10
	11.91344955	-0.33573455	0.99999831	-0.00000066	2.50E-10
	12.67753189	-0.39611536	0.99997860	-0.00000736	3.04E-09
	13.48264892	-0.29694775	1.00000038	-0.00000054	6.90E-11
	14.14241358	-0.43006040	1.00007802	0.00008149	2.54E-08

	125.73060952	-0.33868744	1.00035374	0.00089953	1.76E-08
	126.16812780	-0.21726568	0.99997532	0.00000523	6.34E-10
	126.57000032	-0.30717994	0.99969830	-0.00028769	6.87E-09
◇	126.89863330	-0.61058335	1.24854908	-0.16290432	3.18E-06
	127.21759681	-0.32010287	1.00042752	0.00045232	1.30E-08
	127.68308651	-0.24341398	0.99993610	-0.00000236	2.13E-09
	128.12116088	-0.28389637	1.00010175	-0.00022229	4.95E-09
◇	128.41137217	-0.61577414	1.32422538	-0.11565068	4.11E-06
	128.70334065	-0.30442655	1.00039570	0.00011310	8.78E-09
	129.19732946	-0.26788859	0.99987656	-0.00004493	5.25E-09
	129.67319699	-0.26717842	1.00017817	0.00002664	4.62E-09
◇	129.92927207	-0.60918315	1.33322988	-0.02170382	4.76E-06
	130.18796223	-0.29223540	1.00028313	-0.00012743	6.65E-09
	130.71098079	-0.29045241	0.99983213	-0.00012609	8.19E-09
	131.22717821	-0.25736473	1.00000071	0.00017324	5.54E-09
◇	131.44889208	-0.59054385	1.26610320	0.06973001	4.99E-06
	131.67139581	-0.28429711	1.00010065	-0.00027624	6.60E-09

Table 4. Semiclassical resonances, multiplicities, and error estimates for the three disk scattering problem (A_1 subspace) with $R = 1$, $d = 2.5$ obtained from the signal $C(L)$ with $L < 7.5$ in Fig. 4a. The marked resonances are plotted as diamonds in Fig. 4b.

Re k	Im k	Re d	Im d	ε
4.58122247	-0.08999148	1.00000417	0.00120203	6.97E-08
7.14266960	-0.81391029	1.01834965	-0.00823113	3.51E-06
12.99951105	-0.65166427	1.00042048	-0.00056855	1.31E-06
17.56322689	-0.68356906	0.98459703	-0.03060711	2.28E-05
◇ 18.91024231	-0.78956816	1.03497867	-0.07209360	6.09E-05
27.88792868	-0.54737225	1.02353431	0.00393194	2.30E-05
30.38871017	-0.11367391	1.00121948	0.00747117	2.68E-06
32.09837318	-0.62004177	0.99002266	0.01368255	3.50E-05
36.50721098	-0.38489303	1.00136214	0.01015558	9.58E-06
39.81154707	-0.35977801	1.00778064	-0.00596526	7.00E-05
42.65696984	-0.33910875	0.95316803	0.02942369	1.81E-05
◇ 44.15561123	-0.37442367	0.70366781	-0.27927232	9.13E-05
◇ 45.09670413	-0.31506305	0.77286261	0.10564855	2.54E-05
48.84367280	-0.58547564	0.97205165	0.01832879	3.83E-06
◇ 51.85539738	-0.71582111	1.05998879	-0.22754826	7.06E-05
53.36884896	-0.10779998	1.03903158	-0.03195638	7.48E-06
◇ 57.52623296	-0.37200326	0.54480246	0.04947934	6.95E-05
◇ 60.63258604	-0.84290683	1.12993346	0.06170742	4.50E-05
62.20192292	-0.21464518	1.00384284	0.02041431	3.04E-06
65.68454001	-0.27861785	1.02584325	0.03420385	5.51E-06
67.86305728	-0.29098741	1.01748508	-0.01128120	6.19E-06
◇ 69.32700248	-0.29789188	0.91331209	-0.06283737	5.73E-06
◇ 71.11378807	-0.56166741	1.04431265	0.20817721	4.26E-06
74.85580547	-0.30392250	1.00774480	0.01774683	8.79E-07
77.31348462	-0.31110834	0.98293492	-0.00865456	5.06E-06
◇ 78.74676605	-0.79088169	0.57558136	-0.30381968	1.39E-04
◇ 80.39325912	-0.29001165	0.67726720	-0.02534165	3.99E-05
◇ 83.89182348	-0.48077936	0.83497221	0.04875474	7.22E-05
◇ 85.81836634	-0.41116853	0.97551535	0.10003934	1.05E-05
◇ 88.57708414	-0.62777143	0.72880937	0.41114777	2.73E-05
◇ 93.03487282	-0.12178427	0.98433404	0.07997697	9.37E-05
◇ 97.58490354	-0.41923521	0.98663823	0.14408254	7.12E-05